Proc. R. Soc. Lond. A **425**, 1–16 (1989)
Printed in Great Britain

Curvilinear optical fibre waveguide: characterization of bound modes and radiative field

BY C. Y. H. TSAO AND W. A. GAMBLING, F.R.S.

Optical Fibre Group, Department of Electronics and Computer Science, University of Southampton, Highfield, Southampton SO9 5NH, U.K.

(*Received* 19 *September* 1988)

Optical waveguides have assumed major importance, not only in optoelectronic applications but also, quite recently, in a study of fundamental physical properties of materials. The propagation characteristics of linear optical waveguides, and to a lesser extent those of waveguides curved in a single plane, are well understood. However, optical waveguides having three-dimensional curvature, for example the helical waveguide, have been proposed and fabricated and an analysis of its properties is essential.

In this paper the scalar wave equations for a three-dimensionally curved optical fibre are solved analytically and boundary conditions are applied to the curved core–cladding interface. An asymptotic formula for computing the propagation constant is proposed and the effects of curvilinearity on the characterization of the bound modes are discussed. By using the equivalent fictitious electromagnetic current method, the far radiative field is established and expressions for the radiation losses for various modes are derived.

1. INTRODUCTION

The curvilinear optical waveguide has become increasingly important in fibre optics, sensors, integrated optics, low-birefringence, high-birefringence and many other special optical fibres. The method of analysis is therefore important also. Waveguides having curvatures lying in a single plane have been extensively analysed. The prevailing treatment is to form the scalar wave equation (SWE) in a two-dimensional toroidal coordinate system and it is then possible to obtain approximate expressions for certain selected waveguide parameters, including field deformation, propagation constant correction, radiation loss and bend loss.

However, some recent and important waveguides, for example optical fibres with helical or spiral cores, have curvature in three dimensions. Although the two-dimensional toroidal SWE may be comprehensively modified for the analysis of fibres exhibiting linear birefringence, it is usually necessary to treat circular birefringence, or polarization rotation, by adopting the Tang coordinate system (Lewin *et al.* 1977; Fang *et al.* 1985*a*, *b*; Tsao 1985; Tang 1970). The SWE in the three-dimensional Tang coordinate system is mathematically more rigorous and physically more realistic. True, the variables in the SWE are not separable in either curvilinear coordinate system, but nevertheless it can be assumed that, under certain strict conditions, the electromagnetic wave remains guided; the mode,

however loosely defined, still exists; and its characteristics can be deduced. Despite the non-separation of variables we may still ask whether the rigorous SWE can be solved to obtain more accurate field analyses and radiation studies.

The primary object of this paper is to seek such a solution for the case of single-mode optical fibres. In particular, the paper begins by suggesting an analytic solution for the Tang SWE from which the details of the modal field deformation, together with its effects upon boundary continuities and dispersion, may be studied. To establish the far-field radiation, the so-called equivalent fictitious electromagnetic current (EFC) method is adopted, and the power dissipated by pure bend loss, and other radiations losses, is investigated.

These more rigorous results are compared with those obtained by earlier methods and the practical situations in which they might be applicable are discussed.

2. Modal field in a three-dimensional curved waveguide

Consider a segment of the three-dimensional curved fibre O′–O′ with a core radius a and surrounded by a cladding (figure 1). For any fibre length s (or propagation distance) the fibre centre O must possess normal $\boldsymbol{n}_0$ and binormal $\boldsymbol{b}_0$ vectors that, together with the tangential vector $\boldsymbol{s}_0$, form a trio that evolves down the fibre (Serret–Frenet frame) (Brand 1947; Moon *et al.* 1965). The coordinate system defined by this S.–F. frame is unfortunately oblique because the transverse axes $\boldsymbol{n}_0$ and $\boldsymbol{b}_0$ rotate about the longitudinal axis $\boldsymbol{s}_0$ at a rate of torsion τ. An orthogonal coordinate system is possible only if the transverse axes $\boldsymbol{n}_0'$ and $\boldsymbol{b}_0'$ are chosen such that they rotate at a rate of $-\tau$ against $\boldsymbol{n}_0$ and $\boldsymbol{b}_0$ while remaining stationary with regard to $\boldsymbol{s}_0$ (Tang's frame) as illustrated in figure 2 (Lewin *et al.* 1977; Fang *et al.* 1985*b*; Tsao 1985; Tang 1970). This is the artificial Tang coordinate system, which coexists with the S.–F. coordinates and for which the metric coefficients $h_1 = 1$, $h_2 = r$, $h_3 = 1 - \chi r \cos\theta$, and $\theta = \phi + \psi$ apply. Here (r, ϕ) and (r, θ) are the usual polar coordinates in the S.–F. and Tang's frames, respectively; $\psi = \int -\tau \, \mathrm{d}s$, s is the fibre length, χ is the curvature and $R = 1/\chi$ is the curvature radius that need not be a constant.

In this curved fibre the SWE may be expressed (Fang *et al.* 1985*b*; Tsao 1985; Collin 1960) in equations (1.1) to (1.3).

$$\{\Delta_t + (k^2n^2 - \beta^2)a^2 - \rho^{-2} - 2\beta^2a^2\delta\rho\cos\theta\}\, e_r - (2\rho^{-2}\partial/\partial\phi + \delta\rho^{-1}\sin\theta)\, e_\phi + (2\mathrm{j}\beta a\delta\cos\theta)\, e_s = 0, \quad (1.1)$$

$$\{\Delta_t + (k^2n^2 - \beta^2)a^2 - \rho^{-2} - 2\beta^2a^2\delta\rho\cos\theta\}\, e_\phi + (2\rho^{-2}\partial/\partial\phi + \delta\rho^{-1}\sin\theta)\, e_r - (2\mathrm{j}\beta a\delta\sin\theta)\, e_s = 0, \quad (1.2)$$

$$\{\Delta_t + (k^2n^2 - \beta^2)a^2 - 2\beta^2a^2\delta\rho\cos\theta\}\, e_s - (2\mathrm{j}\beta a\delta\cos\theta)\, e_r + (2\mathrm{j}\beta a\delta\sin\theta)\, e_\phi = 0, \quad (1.3)$$

where $\Delta_t = \partial^2/\partial\rho^2 + \rho^{-1}\partial/\partial\rho + \rho^{-2}\partial^2/\partial\phi^2 - \delta(\cos\theta\,\partial/\partial\rho - \rho^{-1}\sin\theta\,\partial/\partial\phi)$ is the transverse laplacian, $\rho = r/a$ is the normalized radius, $\delta = a/R$ is the 'normalized' curvature, k is the light wave number in free space, n is the refractive index (n_1

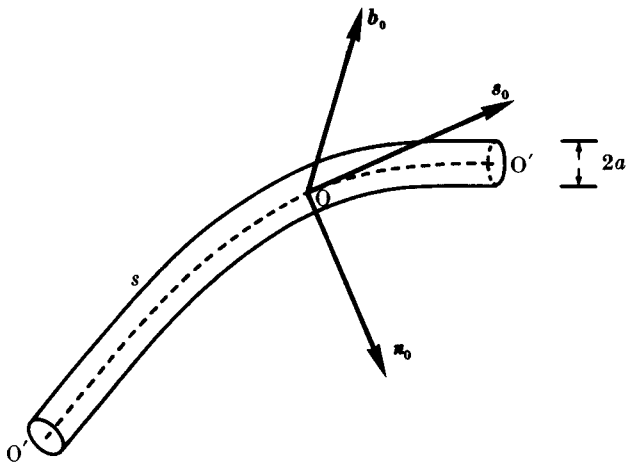

FIGURE 1. A segment of fibre and its normal, binormal and tangential vectors $\boldsymbol{n}_0$, $\boldsymbol{b}_0$ and $\boldsymbol{s}_0$ at any propagation length s.

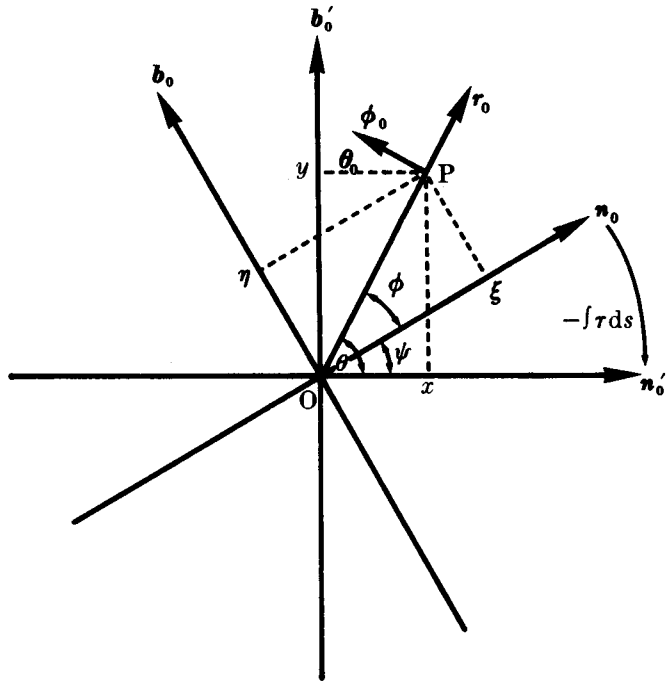

FIGURE 2. The Serret–Frenet coordinates (r, ϕ) or (ξ, η), and Tang's torsionless coordinates (r, θ) or (x, y). Here the unit vectors $\boldsymbol{n}_0$ and $\boldsymbol{b}_0$ are attached to the S.–F. frame; and $\boldsymbol{n}_0'$ and $\boldsymbol{b}_0'$ to the Tang frame.

for the core, n_2 for the cladding), $\beta = \beta_r + j\beta_i$ is the propagation constant in which β_r is the phase factor and β_i the loss factor. The quantities e_r, e_ϕ and e_s are the radial, tangential and axial electric field components ($E = e \exp j\beta s$). A corresponding set of equations can be written for the magnetic components ($H = h \exp j\beta s$) in (1).

Formidable as they may look at first glance, equations (1.1)–(1.3) are certainly not intractable and several key features may be noted. First, the leading term with the curling bracket in (1.1) and (1.2), and modifying e_r and e_ϕ, is the SWE often quoted in two-dimensional toroidal coordinates. It is now followed by additional terms representing couplings from the other two components. Secondly, this cross-component coupling occurs in such a specific manner that there is symmetrical coupling between the radial and tangential fields, both of which also couple to the axial field. Thirdly, the laplacian is modified by a correction factor as a result of the three-dimensional curvature and therefore comprises a further element of self-coupling. These coupling components are important and should not be ignored. This applies particularly to the cross-coupling components because e_r and e_ϕ are always dominant in comparison with e_s (Snyder *et al.* 1983; Love *et al.* 1987; Calvo *et al.* 1987; Fang *et al.* 1985*a*, *b*; Tsao 1985) so that, for instance, the last two terms in (1.3) cannot be neglected without impairing the accuracy. To illustrate the point, consider the following relations, equations (2.1) and (2.2), linking the axial and transverse components in a curved fibre, which may be deduced from the Maxwell equations in general curvilinear coordinates, as given in Appendix A.

$$e_r = \pm(\mathrm{j}\beta a/u^2)[1 \pm 2\beta^2 a^2 \delta\rho\cos\theta/u^2]\{\partial e_s/\partial\rho + k\eta_0\,\partial h_s/\beta\rho\,\partial\phi\}, \tag{2.1}$$

$$e_\phi = \pm(\mathrm{j}\beta a/u^2)[1 \pm 2\beta^2 a^2 \delta\rho\cos\theta/u^2]\{\partial e_s/\rho\,\partial\phi - k\eta_0\,\partial h_s/\beta\,\partial\rho\}. \tag{2.2}$$

Here η_0 stands for the free space characteristic, or intrinsic impedance, $u = U$ and the plus sign is chosen in the core; and $u = W$ and the minus sign is chosen in the cladding, with $U = a\sqrt{(k^2 n_1^2 - \beta^2)}$ and $W = a\sqrt{(\beta^2 - k^2 n_2^2)}$, which are often referred to as the core and cladding phase parameters. Substitution of the transverse laplacian and equations (2.1) and (2.2) into (1.3) yields a scalar wave equation (SWE) involving not only e_s but also h_s. Physically, the term involving h_s represents the coupling effects of the magnetic field h_s upon the electric field e_s. This coupling is negligible in most cases of practical interest and can be excluded from further consideration (Tsao 1985). In comparison with the SWE of a straight waveguide, the resultant SWE derived here will, however, have additional terms from the coupling between the transverse and axial components of the electrical field, which turns out to be $\delta(1 \mp 2\beta^2 a^2/u^2)\{\cos\theta\,\partial/\partial\rho - \rho^{-1}\sin\theta\,\partial/\partial\phi\}\,e_s$. This cross-component coupling contrasts with the simplistic term for self-coupling $(2\beta^2 a^2 \delta\rho\cos\theta)\,e_s$ when cross-coupling is ignored. It can be shown (Tsao 1985) that the self-coupling effects are indeed insignificant for numerous lower-order modes. So we obtain the following for the SWE:

$$\left\{\left(\frac{\partial^2}{\partial\rho^2} + \frac{\partial}{\rho\,\partial\rho} + \frac{\partial^2}{\rho^2\,\partial\phi^2} \pm u^2\right) - \delta\left[\left(1 \mp \frac{2\beta^2 a^2}{u^2}\right)\left(\cos\theta\frac{\partial}{\partial\rho} - \sin\theta\frac{\partial}{\rho\,\partial\phi}\right)\right]\right\} e_s = 0. \tag{3}$$

Having established the proper SWE we are now at the position to solve it. The major steps are outlined in Appendix B and the final results are:

$$\left.\begin{aligned} e_s &= c^e[1 + \delta(\tfrac{1}{2} \mp \beta^2 a^2/u^2)\rho\cos\theta]X(u\rho)/X(u)f, \\ h_s &= c^h[1 + \delta(\tfrac{1}{2} \mp \beta^2 a^2/u^2)\rho\cos\theta]X(u\rho)/X(u)g. \end{aligned}\right\} \tag{4}$$

Here $f = \cos\nu\theta$, $g = -\sin\nu\theta$ (X-polarization), $f = \sin\nu\theta$, $g = \cos\nu\theta$ (Y-polarization) and ν is an integer; $X(u\rho) = J_\nu(U\rho)$ at the core, $X(u\rho) = K_\nu(W\rho)$ at the cladding,

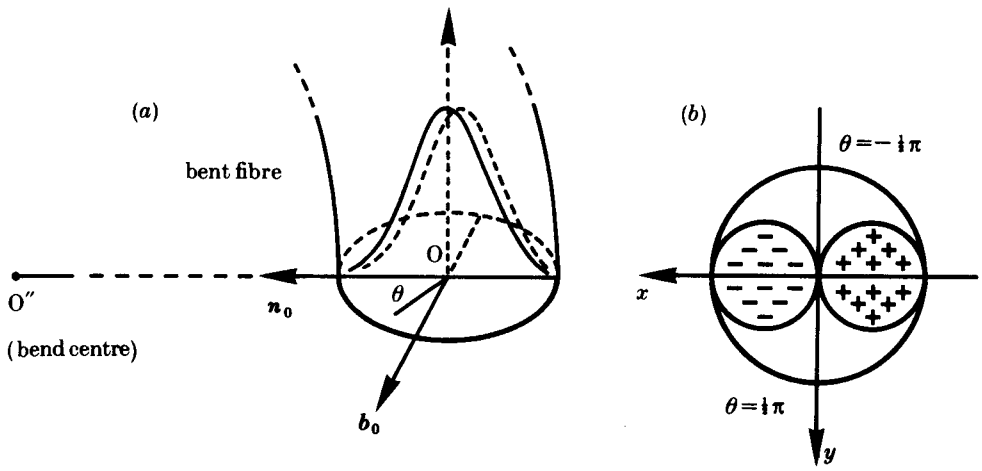

FIGURE 3. (*a*) The field in a bent fibre (dotted line) along the 'normal' axis is deformed in comparison with that in a straight fibre (solid line), with the magnitude proportional to δ. Here $\boldsymbol{n}_0$ and $\boldsymbol{b}_0$ are unit vectors and O″–O the curvature radius. (*b*) The field deformation is also modified by $\cos\theta$ (θ is the azimuthal angle). It is a maximum at $\theta = 0, \pi$, and zero at $\theta = \pm\frac{1}{2}\pi$.

where J and K are Bessel and modified Bessel functions, and c^e and c^h are arbitrary constants to be decided by boundary conditions. A detailed analysis of equation (4), to examine all the features of the axial electromagnetic field would be tedious but the results can be summarized by saying that the curvilinearity 'deforms' the modal field and the amount of relative deformation is $\mp(\beta^2a^2/u^2)\,\delta\rho\cos\theta$ (because of $\beta^2a^2/u^2 \gg 1$), which is proportional to δ and is a maximum when $\theta = 0, \pi$ (figure 3*a*). As might be intuitively expected, the field in the core is weakened inside the bend and strengthened outside; although the trend is reversed at the cladding but the field on the whole has been 'shifted'. The function of the angular modifier $\cos\theta$ is to make this shift fall to zero as θ moves towards the neutral plane of the bend ($\theta = \pm\frac{1}{2}\pi$, see figure 3*b*). The field deformation determines the curvilinear fibre behaviour, and is bound to have some impact on the modal characterizations.

3. BOUNDARY CONTINUITY

The continuity condition governing the tangential electromagnetic field components at the core–cladding interface must hold even when the fibre axis becomes curved (Stratton 1941). To apply these continuities we must handle the tangential, rather than the axial, field components because, for the reason mentioned earlier, the latter are negligibly small. Failure to do so inevitably results in fundamental errors in the discussion that follows.

Note that

$$\left.\begin{aligned}\frac{\partial e_z}{\partial\rho} &= c^e\left[\frac{uX(u\rho)}{X(u)}\right]\left\{1-\beta^2a^2u^{-2}\left[\frac{X(u\rho)}{u\rho X'(u\rho)}+1\right]\cos\theta\right\}f,\\ \frac{\partial h_z}{\partial\rho} &= c^h\left[\frac{uX(u\rho)}{X(u)}\right]\left\{1-\beta^2a^2u^{-2}\left[\frac{X(u\rho)}{u\rho X'(u\rho)}+1\right]\cos\theta\right\}g,\end{aligned}\right\} \tag{5}$$

$$\left.\begin{aligned}\frac{\partial e_s}{\partial \phi} &= c^e\left[\frac{X(u\rho)}{X(u)}\right](1-\beta^2a^2\delta\rho\cos\theta/u^2)\,g,\\ \frac{\partial h_s}{\partial \phi} &= c^h\left[\frac{X(u\rho)}{X(u)}\right](1-\beta^2a^2\delta\rho\cos\theta/u^2)f.\end{aligned}\right\} \tag{6}$$

The transverse field may now be formulated straight away by substitution of (5) and (6) into (2) even without solving equations (1.1)–(1.2) (see table 1 for detail). Having obtained e_ϕ and h_ϕ, it is simple to eliminate the coefficients c^e and c^h. This gives rise to equation (7):

$$\begin{aligned}&\pm\nu(U^{-2}+\beta^2a^2U^{-4}\delta\cos\theta+W^{-2}-\beta^2a^2W^{-4}\delta\cos\theta)\\ &\quad=(J'/UJ)(1+\beta^2a^2U^{-2}\delta\cos\theta)-\beta^2a^2U^{-4}\delta\cos\theta\\ &\qquad+(K'/WK)(1-\beta^2a^2W^{-2}\delta\cos\theta)+\beta^2a^2W^{-4}\delta\cos\theta.\end{aligned} \tag{7}$$

TABLE 1. FIELD COMPONENTS AND BOUNDARY CONTINUITY CONDITIONS FOR HE/EH MODES

(Boundary continuity condition is equation (8).)

e_r	$Uf_\nu\{X_{\nu-1}(u\rho)+\beta^2a^2\delta\rho\cos\theta X'_\nu(u\rho)/u^2\}/uX_\nu(u)$
e_ϕ	$Ug_\nu\{X_{\nu-1}(u\rho)+\beta^2a^2\delta\rho\cos\theta X'_\nu(u\rho)/u^2\}/uX_\nu(u)$
e_s	$Uf_\nu X_\nu(u\rho)\{1\mp\beta^2a^2\delta\rho\cos\theta/u^2\}/\mathrm{j}\beta aX_\nu(u)$
h_r	$-Ug_\nu Y_1\{X_{\nu-1}(u\rho)+\beta^2a^2\delta\rho\cos\theta X'_\nu(u\rho)/u^2\}/uX_\nu(u)$
h_ϕ	$Uf_\nu Y_1\{X_{\nu-1}(u\rho)+\beta^2a^2\delta\rho\cos\theta X'_\nu(u\rho)/u^2\}/uX_\nu(u)$
h_s	$-Ug_\nu Y_1 X_\nu(u\rho)\{1\mp\beta^2a^2\delta\rho\cos\theta/u^2\}/uX_\nu(u)$

Here, $J=J_\nu(U), K=K_\nu(W)$, the prime attached to J and K denoting the derivative; the symbol '$\pm$' may be '+' or '−' depending on which mode is referred to. For HE_ν and EH_ν modes, the obvious relations $J'_\nu=J_{\nu-1}-\nu J_\nu/U$; $K'_\nu=-K_{\nu-1}-\nu K_\nu/W$ and $J'_\nu=-J_{\nu+1}+\nu J_\nu/U$; $K'_\nu=-K_{\nu-1}+\nu K_\nu/W$ may be adopted to deduce (8):

$$\begin{aligned}&(J_{\nu\mp1}/UJ_\nu)(1+\beta^2a^2U^{-2}\delta\cos\theta)\mp\beta^2a^2U^{-4}\delta\cos\theta\\ &\qquad=\pm(K_{\nu\mp1}/WK_\nu)(1-\beta^2a^2W^{-2}\delta\cos\theta)\mp\beta^2a^2W^{-4}\delta\cos\theta.\end{aligned} \tag{8}$$

In (8) and throughout the remainder of the paper the argument of J_ν is always U and of K_ν is always W. Equations (7) and (8) are the equivalent of the ordinary eigenvalue equation (EVE). The term is not applied to them here because of the inclusion of the explicit θ-dependence, but equations (7) and (8) still depict exactly how the propagation constant should be 'readjusted' so as to maintain the deformed modal field. This is known as the phase factor correction problem (Chang *et al.* 1976), which can now be solved, for the first time, for arbitrarily curved core–cladding boundary continuities, provided (7) and (8) can be solved.

4. ASYMPTOTIC FORMULA FOR THE U-PARAMETER

Equations (8) are in transcendental form, for which the solutions can only be sought numerically. An analytic solution would, of course, be attractive in

allowing an easy assessment of a range of waveguide parameters, including phase factor correction, linear birefringence, group velocity and dispersion. An approximate expression can be obtained which is valid asymptotically. To this end we shall now consider the cases $V \gg 1$, $U \ll V$, and $W \approx V$. The symbol V denotes the normalized frequency of a cylindrical optical fibre and is given by $V^2 = U^2 + W^2 = a^2k^2(n_1^2 - n_1^2) = 2\Delta a^2k^2n^2$, where $\Delta = (n_1^2 - n_2^2)/2n^2 \approx (n_1 - n_2)/n_1$ is the relative core/cladding index difference (in practice $\Delta \approx 0.01$).

For sufficiently large values of V, the fibre becomes multimoded, the cut-off condition V_c for the second-order modes depending on the type of waveguide and its configuration. Thus $V_c = 2.4$ in a straight optical fibre with a constant refractive index in the core and a uniform cladding. However, if the fibre axis is curved the radiation loss of the second-order modes near cut-off rises rapidly and the effective cut-off value is greatly increased. Thus, in a typical fibre having a helical core, of the kind considered in this paper, the effective V_c is increased by more than an order of magnitude. Thus in a curved fibre, single-mode operation can be obtained at relatively large V values, but nevertheless the formulae derived in the remainder of this section are approximate when V is small. This point is discussed further in §9. With the above assumptions, some terms in (8) become insignificant and it can therefore be rewritten as

$$(J_{\nu\mp1}/UJ_\nu)(1 + pV^2/U^2) = \pm[K_{\nu\mp1}/WK_\nu + pV^2/U^4], \tag{9}$$

where $p = (\delta/2\Delta)\cos\theta$. Differentiating both sides of (9), with the help of

$$W\,dW = V\,dV - U\,dU,$$

$$\left(1 + \frac{pV^2}{U^2}\right)\left(\frac{J_{\nu\mp1}}{UJ_\nu}\right)' \pm \left(\frac{U}{W}\right)\left(\frac{K_{\nu\mp1}}{WK_\nu}\right)' = \mp\frac{1}{U}\left(1 + \frac{pV^2}{U^2}\right)$$

and

$$\frac{J_{\nu\mp1}}{UJ_\nu} = \left(\pm\frac{K_{\nu\mp1}}{WK_\nu} \pm \frac{pV^2}{U^4}\right)\left(1 - \frac{pV^2}{U^2}\right),$$

results in the expression

$$\frac{dU}{dV} \approx \left[-\left(1 - \frac{K_{\nu\mp1}^2}{K_\nu K_{\nu\mp2}}\right)\frac{VK_{\nu\mp2}}{W^2K_\nu} \mp \frac{2pVK_{\nu\mp1}}{U^2WK_\nu} \pm \frac{2pV}{U^4}\right] \Bigg/ \left[\mp\frac{1}{U}\left(1 + \frac{pV^2}{U^2}\right) \mp \frac{2pV^2K_{\nu\mp1}}{U^3WK_\nu} \pm \frac{4pV^2}{U^5}\right]$$

or

$$dU/dV \approx (U/V^2)[1 + pV^2(1 - 2V/U^2)/U^2]. \tag{10}$$

Use has also been made of the following asymptotic approximations:

$$K_{\nu-2}/WK_\nu \approx K_{\nu-1}/WK_\nu \approx 1/V,$$

$$1 - K_{\nu-1}^2/K_\nu K_{\nu-2} \approx 1/V.$$

Equation (10) is the differentiation relation relating the U-parameter to the V-value of a fibre and is, of course, helpful for estimating dispersive parameters, as

will be made clear shortly. A more useful U-parameter formula is given by (11) which is the integration of (10).

$$U \approx U_{j\nu i} \exp\{-[1-pV^2(1-V/U_{j\nu i}^2)/U_{j\nu i}^2]/V\}. \tag{11}$$

Here $U_{j\nu i}$ is the ith zero of J_ν, and $\nu = 0, 1, 2, 3$ for HE_1, $TE_0/TM_0/HE_2$, EH_1 and EH_2 modes, respectively. The virtue of this asymptotic U-parameter formula is that with a given fibre design specified by its V-value, and a curved geometry, it always enables one to work out the correction for U and therefore β_r, which is very convenient. We shall take dispersive parameters (group velocity and dispersion) as examples to show how this is done.

5. Group velocity and dispersion of a curved fibre

For a curved fibre, the group (normalized) velocities $V_g(V_{Ng})$, and the dispersion, are dependent on the differential relation between U and V in (10). Thus, the group velocities and the dispersion will immediately become defined as soon as $dU/dV = F(V)$ is known, as will be shown.

The group velocity is defined through $1/v_g = d\beta/d\omega$. Here ω is the light circular frequency, $d\omega = -\omega\, d\lambda/\lambda$, λ is the light wavelength in free space; $d\beta = (kn_1^2\, dk + k^2 n_1\, dn_1 - U\, dU/a^2)/\beta$ and $dk/k = -d\lambda/\lambda$. Putting all these together we find

$$\frac{1}{v_g} = \left(\frac{1}{\omega\beta}\right)\left\{k^2 n_1^2 + U\lambda F(V)\frac{dV}{a^2\, d\lambda} - k^2 n_1^2 \frac{\lambda\, dn_1}{n_1\, d\lambda}\right\}. \tag{12}$$

It is emphasized that every term in the above curling bracket has a clear physical meaning. For example, the last term is zero in non-dispersive materials and its contribution is known as the material dispersion. The first term, however, is present even for non-dispersive materials because it is proportional to the index squared. The second term is associated with the waveguide mechanism that may be further clarified through $dV/dk = V\{1/k + d\ln(n_1^2 - n_2^2)/2dk\}$, or $dV/d\lambda = V\{-1/\lambda + d\ln(n_1^2 - n_2^2)/2d\lambda\}$. Thus, equation (12) may be written

$$\frac{1}{v_g} = \left(\frac{kn_1}{\beta c_0}\right)\left\{1 + \left[\frac{UF(V)\,\lambda}{Vn_1}\right]\left[\frac{d(n_1 - n_2)}{d\lambda}\right] - \frac{\lambda\, dn_1}{n_1\, d\lambda}\right\}, \tag{12.1}$$

where c_0 is the velocity of light in a vacuum and

$$F(V) = (U/V^2)[1 + pV^2(1 - 2V/U^2)/U^2],$$

which is close enough to unity for most cases of practical interest. This is the group velocity formula from which the normalized group velocity v_{Ng} and the dispersion $d^2\beta/d\omega^2$ may be formulated; and the curvilinearity effects may be identified. Thus;

$$\frac{1}{v_{Ng}} = \left(\frac{kn_1}{\beta}\right)\left\{1 + \left(\frac{UF\lambda}{Vn_1}\right)\left(\frac{dn_1}{d\lambda} - \frac{dn_2}{d\lambda}\right) - \frac{\lambda\, dn_1}{n_1\, d\lambda}\right\}, \tag{12.2}$$

$$\frac{d^2\beta}{d\omega^2} = \left(\frac{\lambda}{\omega c_0}\right)\left\{\frac{\lambda\, d^2 n_1}{d\lambda^2} - \left(\frac{\lambda UF}{V}\right)\left(\frac{d^2 n_1}{d\lambda^2} - \frac{d^2 n_2}{d\lambda^2}\right) - \left(\frac{dn_1}{d\lambda} - \frac{dn_2}{d\lambda}\right)\frac{d(\lambda UF/V)}{d\lambda}\right\}. \tag{12.3}$$

It is readily seen from (12) that the curved geometry slightly modifies the waveguide dispersion.

6. Linear birefringence

The phase factor correction and the asymptotic U formula fail to predict the phase difference between the two polarizations (linear birefringence). This is because the phase factor corrections are accurate to the order of δ while the polarization phase difference correction is proportional to δ^2. Nevertheless, the linear birefringence can be directly determined from the detailed field deformation, as illustrated in Appendix C.

7. Losses and equivalent fictitious currents (EFC)

A curvilinear waveguide is lossy and the modal propagation constant must therefore be complex. Several factors may contribute to losses, including a finite cladding, mode conversion from one segment to the next resulting from the variations of curvature, and radiation (Gambling *et al.* 1976, 1977, 1978*a*, *b*, 1979; Mercatili 1969; Shevchenko 1971; Gloge 1972; Arnaud 1974; Miyagi *et al.* 1976). This paper is concerned with the additional radiation effects caused by three-dimensional curvature.

To investigate radiation conditions we need to establish the radiation field in a curved fibre, which may be written

$$\nabla \times \boldsymbol{E} = \boldsymbol{J}_{\mathrm{m}} + \mathrm{j}\eta_0 k\boldsymbol{H}, \tag{13.1}$$

$$\nabla \times \boldsymbol{H} = \boldsymbol{J}_{\mathrm{e}} - \mathrm{j}Y_0 kn^2\boldsymbol{E}. \tag{13.2}$$

Here, Y_0 is the characteristic admittance of vacuum ($1/\eta_0$), and $\boldsymbol{J}_{\mathrm{m}}$ and $\boldsymbol{J}_{\mathrm{e}}$ are the equivalent fictitious magnetic and electric currents (EFC) resulting from the difference of the rot operator ∇ in three-dimensional curved and straight coordinates (C. Y. H. Tsao, unpublished work; Collin 1960; Stratton 1941). These currents do not exist in practice, but they are convenient for demonstrating and computing the equivalent radiation field. Term $-\mathrm{j}Y_0 k(n_1^2 - n_2^2)\boldsymbol{E}$ in (13.2) is normally taken to be the source of 'pure' bend loss (Lewin 1974; Marcuse 1976*a*, *b*; Marcuse 1972; Snyder *et al.* 1983; Love *et al.* 1987; Calvo *et al.* 1987). However, equations (13.1) and (13.2) indicate that there are in addition the equivalent currents, $\boldsymbol{J}_{\mathrm{m}}$ and $\boldsymbol{J}_{\mathrm{e}}$, which also radiate and add to the radiation loss.

Adopting the notations $\boldsymbol{J}_{\mathrm{m}} = \boldsymbol{j}_{\mathrm{m}} \exp \mathrm{j}\beta s$ and $\boldsymbol{J}_{\mathrm{e}} = \boldsymbol{j}_{\mathrm{e}} \exp \mathrm{j}\beta s$ and neglecting the insignificant axial component we may write

$$\boldsymbol{j}_{\mathrm{m}} = \mathrm{j}\beta\delta\rho\cos\theta \quad (\boldsymbol{r}_0 e_\phi - \boldsymbol{\theta}_0 e_r), \tag{14.1}$$

$$\boldsymbol{j}_{\mathrm{e}} = \mathrm{j}\beta\delta\rho\cos\theta \quad (\boldsymbol{r}_0 h_\phi - \boldsymbol{\theta}_0 h_r), \tag{14.2}$$

where $\boldsymbol{r}_0$ and $\boldsymbol{\theta}_0$ are unit radial and tangential vectors in the Tang's coordinate; and e_r, h_r, e_ϕ and h_ϕ are the relevant electromagnetic fields in the curved waveguide. We are particularly keen on 'visualizing' these currents for a typical X- or Y-polarization. With a little mathematical manipulation one can easily verify equations (15) and (16).

X-polarization:

$$\boldsymbol{j}_{x\mathrm{m}} = -\mathrm{j}\beta\delta\rho\Gamma\cos\theta\boldsymbol{y}_0', \tag{15.1}$$

$$\boldsymbol{j}_{x\mathrm{e}} = \mathrm{j}\beta\delta\rho\Gamma Y_1\cos\theta\boldsymbol{x}_0'; \tag{15.2}$$

Y-polarization:

$$j_{ym} = \mathrm{j}\beta\delta\rho\Gamma\cos\theta x'_0, \tag{16.1}$$

$$j_{ye} = \mathrm{j}\beta\delta\rho\Gamma Y_1\cos\theta y'_0. \tag{16.2}$$

Here, $Y_1 = n_1 Y_0$, x'_0 and y'_0 are the normal and binormal vectors, and Γ is taken as $J_0(U\rho)/J_1(U)$ because the deformation correction is not essential in this problem. Figure 4*a*, *b* qualitatively shows the orientations of the EFC distributions for the two orthogonal polarizations, from which it can be seen that $-\mathrm{j}Y_0 k(n_1^2-n_2^2)\boldsymbol{e}$ and the EFCs could be characterized as 'monopole' and 'dipole' currents (Kraus 1950).

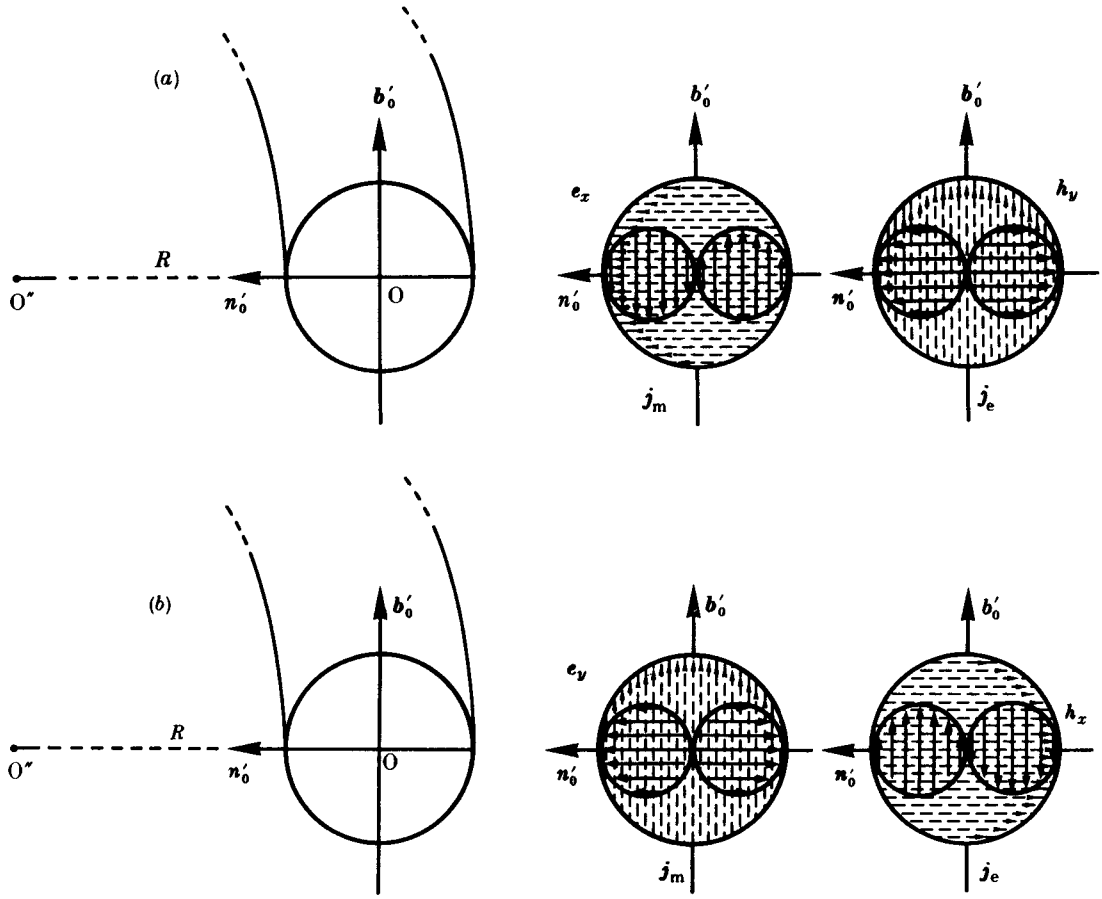

FIGURE 4. Equivalent fictitious magnetic and electric currents j_m and j_e (solid lines) together with the electric $\boldsymbol{e}$ or magnetic $\boldsymbol{h}$ fields (dotted lines) (*a*) for x-polarization and (*b*) for y-polarization.

8. RADIATION FROM ELECTROMAGNETIC EFCS

Radiation from EFCs are perfectly symmetric for both the X- and Y-polarizations. The X-polarization will be taken as an example to illustrate the radiation condition and consequent losses arising from electromagnetic EFCs. We

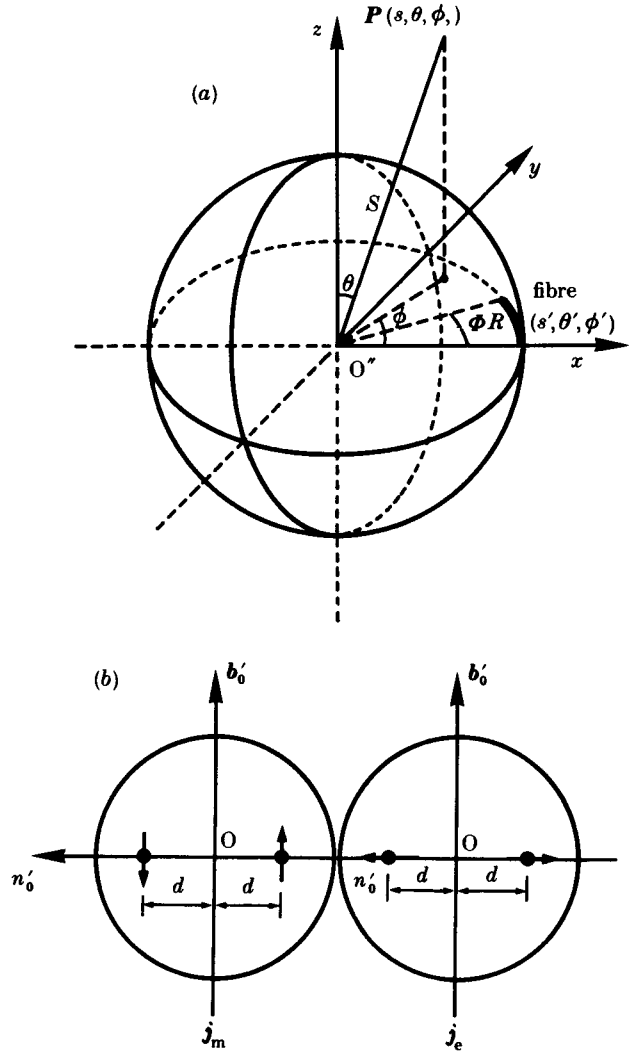

FIGURE 5. (*a*) The spherical coordinates of a short segment of fibre (s', θ', ϕ') and 'target' coordinate (s, θ, ϕ). (*b*) The EFCs j_m and j_e are modelled by the dipole line current source with a separation 2d.

ignore additional effects of the finite core cross section (see p. 480 of Snyder *et al.* 1983) and model these EFCs as line dipoles carrying a total current of

$$I_{0m} = \int\int \beta\delta\rho\Gamma \cos\theta r \, \mathrm{d}r \, \mathrm{d}\theta = \frac{4\beta a^3}{3RU}, \quad I_{0e} = Y_1 I_{0m},$$

with a dipole separation

$$2d = 2\int \Gamma r^2 \, \mathrm{d}r \Big/ \int \Gamma r \, \mathrm{d}r \approx \tfrac{4}{3}a.$$

A segment of this line current source is placed in a spherical coordinate system so that its binormal coincides with z_0; and

$$\boldsymbol{I}_{\mathrm{m}}(\boldsymbol{P}') = I_{0\mathrm{m}} \exp(\mathrm{j}R\beta\phi')\, z_0\{\delta[S'-(R+d)]-\delta[S'-(R-d)]\}\,\delta(\theta'-\tfrac{1}{2}\pi)/S\} \text{ for } \phi' \leqslant \boldsymbol{\Phi},$$

or zero otherwise (figure 5*a*, *b*). The magnetic vector potential $\boldsymbol{A}_{\mathrm{m}}$ is well known as

$$\boldsymbol{A}_{\mathrm{m}} = \iiint_{v'} \boldsymbol{I}_{\mathrm{m}}(\boldsymbol{P}')\, G(\boldsymbol{P}, \boldsymbol{P}')\, \mathrm{d}v', \tag{17}$$

where $G(\boldsymbol{P}, \boldsymbol{P}') = \exp[\mathrm{j}kn_2(S - S'\cos\kappa)]/4\pi S$ is the Green function, $\cos\kappa = \cos\theta\cos\theta' + \sin\theta\sin\theta'\cos(\phi-\phi')$; and $\mathrm{d}v' = (S')^2 \sin\theta'\,\mathrm{d}S'\,\mathrm{d}\theta'\,\mathrm{d}\phi'$. (Here all spherical 'source' coordinates (S', θ', ϕ'), and 'target' coordinates (S, θ, ϕ) should not be confused with the same symbols for the polar coordinates used in earlier sections.) Note (Whittaker *et al.* 1935)

$$\exp[-\mathrm{j}z\theta] = \int_{-\infty}^{\infty} \exp[\mathrm{j}q(-\tfrac{1}{2}\pi+\theta)]\, J_q(z)\,\mathrm{d}q \tag{18.1}$$

and the δ-function property (Jones 1966)

$$\delta[f(x)] = \delta(x)/|f'(x)|. \tag{18.2}$$

By using these identities, the integration in (17) may be easily carried out to give

$$\boldsymbol{A}_{\mathrm{m}} = [\exp(\mathrm{j}kSn_2)/4\pi S]\, z_0\, 2\pi I_{0\mathrm{m}} R \exp[\mathrm{j}\beta R(\phi-\tfrac{1}{2}\pi)] \{(d/R)[1+2(q^2-z^2)^{1.5}/3q^2)]\}\, J_q(z). \tag{19}$$

Here $q = \beta R$ and $z = kn_2 R\sin\theta$. The radiation field is associated with $\boldsymbol{A}_{\mathrm{m}}$ in the manner $\boldsymbol{e}_{\mathrm{m}} = \nabla \times \boldsymbol{A}_{\mathrm{m}}$, and $h_{\mathrm{m}} = -\mathrm{j}kn_2^2\, Y_0\{\boldsymbol{A}_{\mathrm{m}} + \nabla(\nabla\cdot\boldsymbol{A}_{\mathrm{m}})/k^2n_2^2\}$, from which the Poynting vector, together with the power dissipation, may be computed. The electric potential vector $\boldsymbol{A}_{\mathrm{e}}$ may be treated in much the same way so that the total power loss may be calculated. The power attenuation coefficient $2\beta_{\mathrm{i}}$ is then given by

$$2\beta_{\mathrm{i}} = \{\tfrac{2}{27}(\delta/\pi\Delta)^2[\delta + 4\Delta W^3/3V^2]^2 + b\}\,\alpha \tag{20}$$

and

$$\alpha = [(\sqrt{(\pi W)}\, V^2)/(2\sqrt{(aR)}\, U^2)] \exp(-4\Delta W^3/3\delta V^2). \tag{21}$$

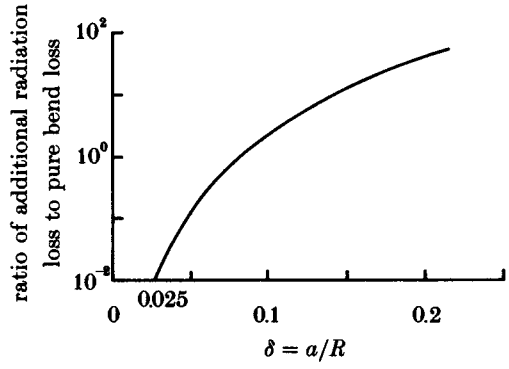

FIGURE 6. The ratio of the additional dipole radiation to the pure bend loss as a function of δ, for a typical single-mode fibre in which $V = 2.4$, $a = 5\ \mu\mathrm{m}$, and $\Delta = 5.5 \times 10^{-4}$.

In the above equations α is the bend loss factor caused by the monopole radiation, and $b = 1$, or 0.5, for the Y- or X-, polarizations, respectively. Existing theories give the power attenuation coefficient as $2\beta_i = b\alpha$. The remaining term in (20) represents the additional dipole radiation predicted by the more comprehensive theory described here. The magnitude of the effect is illustrated in figure 6, where the ratio of the additional loss to the pure bend loss is plotted as a function of the relative bend radius. It can be seen that, in practice, the additional radiation loss is small compared with the pure bend loss, except when $\delta \gg \Delta$.

9. Concluding remarks

The SWE has been solved analytically for a general three-dimensional curvilinear Tang's coordinate system. The method used in this paper is stringent and accurate yet the complication usually associated with mathematical rigour seems bearable. From this solution the electromagnetic waves are characterized, the boundary continuities on a general curved core–cladding interface are applied, an asymptotic formula for calculating the U-parameter is proposed; and the curvilinearity effects upon propagation constant, waveguide group velocity or dispersion, linear birefringence, etc. are derived. In addition, the far-field radiation field has also been investigated by the EFC method. It is found that in addition to the usual pure bend loss there is an additional source of radiation which originates from the peculiar form of the rot operator in the Tang's coordinate. This added power loss appears to be insignificant for most practical cases but it could become important for waveguides when they are strongly curved.

The above analysis indicates that some refinements are necessary to the conventional analyses of optical fibre properties. However, it is also important to estimate the magnitude of the corresponding corrections in practical situations. For example, single-mode fibres are operated with $V \leqslant 2.4$ whereas the analysis in §4 assumes $V \geqslant 1$. However, the error in cases where $V = 2.4$ is small, and is only 8% even when V is as low (Snyder *et al.* 1983) as 1.4.

For a typical helical fibre made in our laboratory, for which $V = 2.4$, $a = 5\ \mu\text{m}$, $\Delta = 5.5 \times 10^{-4}$, with a core offset of 80 μm and a pitch length of 0.5 mm, the additional radiation loss predicted by the theory given above is a few per cent of the normal bend loss. As with other types of bend loss the effect increases rapidly at high rates of curvature so that for a core offset and a pitch length of 32 μm, and 0.2 mm, respectively the additional loss becomes comparable with the other bend losses. Such a tight helix is unlikely to be of practical importance, however.

Similarly, a straight single-mode fibre with $V = 2.4$, $a = 1.2\ \mu\text{m}$ and $\Delta = 0.01$ at $\lambda = 0.633\ \mu\text{m}$ has a value of $F(V) = U/V^2 \approx 0.28$. If such a fibre is drawn as a helix with an offset of 80 μm and a pitch length of 1.5 mm then $F(V)$ is changed to 0.24, so that the dispersion given by equation (12) is not altered significantly.

It would appear, therefore, that in most cases of practical importance the required corrections are small and existing analyses are sufficiently accurate.

This work has been done under the auspices of the Science and Engineering Research Council and this support is sincerely acknowledged. The authors also thank C. D. Hussey, P. St-J. Russell, M. C. Farries, P. Harris and P. Morkel for many useful discussions.

Appendix A. Relation between transverse and axial fields in a general curvilinear coordinate

$$\boldsymbol{e}_t = \mathrm{j}\{\beta'\nabla_t e_s - \sqrt{(\mu/\epsilon_0)}\, k\boldsymbol{s}_0 \times \nabla_t h_s\}/(k^2n^2 - \beta'^2),$$

$$\boldsymbol{h}_t = \mathrm{j}\{\beta'\nabla_t h_s + \sqrt{(\epsilon_0/\mu)}\, kn^2\boldsymbol{s}_0 \times \nabla_t e_s\}/(k^2n^2 - \beta'^2),$$

where $\beta' = \beta(1+\delta\rho\cos\theta)$; and μ and ϵ_0 are free space magnetic permeability and electric permittivity, respectively.

Appendix B. Solution of equation (3)

Letting $e_s = Y_0^e + \delta Y_1^e$ and reorganizing terms of power δ of equation (3), we may have

$$\{\partial^2/\partial\rho^2 + \rho^{-1}\partial/\partial\rho + \rho^{-2}\partial^2/\partial\phi^2 \pm u^2\}\, Y_0^e = 0, \tag{B 1}$$

$$\left\{\frac{\partial^2}{\partial\rho^2} + \frac{\partial}{\rho\,\partial\rho} + \frac{\partial^2}{\rho^2}\partial\phi^2 \pm u^2\right\} Y_1^e = \left\{\left(1 \mp \frac{2\beta^2a^2}{u^2}\right)\cos\theta\left(\frac{\partial}{\partial\rho} - \tan\theta\frac{\partial}{\rho\,\partial\phi}\right)\right\} Y_0^e. \tag{B 2}$$

Equation (B 1) is the straight fibre SWE for which the solution is well known: $Y_0^e = c^e X_\nu(u\rho) f_\nu$, with c^e being a constant, $f_\nu = \cos\nu\theta$ or $\sin\nu\theta$ (an integer ν), and $X_\nu(u\rho)$ being Bessel and modified Bessel functions. The solution of (B 2) is $Y_1^e = c^e(\frac{1}{2} \mp \beta^2a^2/u_2)\,\rho\cos\theta X_\nu(u\rho) f_\nu$, of which the validity may be authenticated by a straightforward substitution.

By combining these two terms the solutions summarized in equations (4) are easily envisaged.

Appendix C. Linear birefringence caused by a three-dimensional curved geometry

It is now convenient to refer to the SWE of a cartesian Tang's coordinate and re-express them in (C 1) and (C 2) (Fang *et al.* 1985):

$$(\Delta_t + k^2n^2 - \beta_\xi^2)\, e_\xi = -\chi^2\sin\psi\cos\psi e_\eta/h^2 - \{\mathrm{j}\beta 2\chi\cos\psi/h^2 + \chi^2\cot\sigma\sin\psi/h^2 + \chi^3\cot\sigma\cos\psi\,\Xi/h^3\}\, e_s, \tag{C 1}$$

$$(\Delta_t + k^2n^2 - \beta_\eta^2)\, e_\eta = -\chi^2\sin\psi\cos\psi e_\xi/h^2 + \{\mathrm{j}\beta 2\chi\sin\psi/h^2 - \chi^2\cot\sigma\cos\psi/h^2 + \chi^3\cot\sigma\sin\psi\Xi/h^3\}\, e_s, \tag{C 2}$$

where

$$\beta_\xi^2 = \beta^2/h^2 + \chi^2\cos^2\psi/h^2 - \mathrm{j}\beta\chi^2\cot\sigma\,\Xi/h^3,$$

$$\beta_\eta^2 = \beta^2/h^2 + \chi^2\sin^2\psi/h^2 - \mathrm{j}\beta\chi^2\cot\sigma\,\Xi/h^3,$$

$$\Xi = \xi\sin\psi + \eta\cos\psi,\ \cot\sigma = \tau/\chi,\ h = h_3,$$

and (ξ, η) are the S.–F. frame normal and binormal axes. The birefringence we are looking for is defined as the propagation constant difference between two orthogonal polarizations which may make sense only in Tang's axes (x, y) (see

figure 2). We note, however, that (x, y) may overlap with (ξ, η) at $\psi = \frac{1}{2}m\pi$ ($m = 4n$, m and n are integers), and this gives rise to (C 3) and (C 4).

$$(\Delta_t + k^2n^2 - \beta_x^2)\, e_x^x = -(\mathrm{j}\beta 2\chi/h^2 + \chi^3 r \cot\sigma \sin\theta/h^3)\, e_s^x, \tag{C 3}$$

$$(\Delta_t + k^2n^2 - \beta_y^2)\, e_y^y = -(\chi^2 \cot\sigma/h^2)\, e_s^y. \tag{C 4}$$

Here superscripts 'x' and 'y' denote polarization axes, and

$$e_x^x = e_y^y = U\{X_0(u\rho) + X_1'(u\rho)\,\beta^2a^2\delta\rho\cos\theta/u^2\}/uX_1(u), \tag{C 5}$$

$$e_s^x = UX_1(u\rho)\{1 - \beta^2a^2\delta\rho\cos\theta/u^2\}\cos\theta/[\mathrm{j}\beta aX_1(u)], \tag{C 6}$$

$$e_s^y = UX_1(u\rho)\{1 - \beta^2a^2\delta\rho\cos\theta/u^2\}\sin\theta/[\mathrm{j}\beta aX_1(u)] \tag{C 7}$$

(see table 1). To get $(\beta_y^2 - \beta_x^2)$, the integral

$$\int_0^\infty \int_0^{2\pi} [e_y^y(\Delta_t + k^2n^2 - \beta_x^2)\, e_x^x - e_x^x(\Delta_t + k^2n^2 - \beta_y^2)\, e_y^y]\,\mathrm{d}A$$

may be carried out, where $\mathrm{d}A = a^2\rho\,\mathrm{d}\rho\,\mathrm{d}\theta$. In view of

$$\iint [e_y^y \Delta_t e_x^x - e_x^x \Delta_t e_y^y = \oint_l [e_y^y \nabla_t e_x^x - e_x^x \nabla_t e_y^y]\, n\,\mathrm{d}l = 0 \quad (\text{for } \rho \to \infty),$$

and

$$\iint e_x^x e_s^y \chi^2 \cot\sigma\,\mathrm{d}A/h = 0$$

$$\iint -e_y^y e_s^x \chi^3 r \cot\sigma \sin\theta\,\mathrm{d}A/h^3 = 0,$$

we arrive at

$$(\beta_y^2 - \beta_x^2) \iint e_y^y e_x^x\,\mathrm{d}A = -\iint 2\mathrm{j}\beta\chi\, e_y^y e_s^x\,\mathrm{d}A. \tag{C 8}$$

It can be shown that

$$\iint e_y^y e_x^x\,\mathrm{d}A = \pi a^2V^2/W^2, \tag{C 9}$$

$$\iint -2\mathrm{j}\beta\chi\, e_y^y e_s^x\,\mathrm{d}A = 0.5\delta^2\beta^2a^2U^2\left\{\left(\frac{1}{U^4} - \frac{1}{W^4}\right) - \left(\frac{J_0J_2}{U^4J_1^2} - \frac{K_0K_2}{W^4K_1^2}\right)\right\} \tag{C 10}$$

and, therefore, the birefringence takes the following form:

$$\Delta\beta_{yx} = (\beta_y - \beta_x) = 0.25\delta^2\beta\left\{\left(\frac{W^2 - U^2}{U^2W^2}\right) + \frac{1}{V^2}\left(\frac{U^2K_0K_2}{W^2K_1^2} - \frac{W^2J_0J_2}{U^2J_1^2}\right)\right\}. \tag{C 11}$$

The amount of birefringence predicted by (C 11) is insignificant in most practical interest, in particular in presence of stress in bent fibres.

References

Arnaud, J. A. 1974 *Bell System tech. J.* **53**, 1379–1397.

Brand, L. 1947 *Vector and tensor analysis*. New York: John Wiley. London: Chapman & Hall.

Calvo, M. L. & Alvarez-Estrada, R. F. 1987 *J. opt. Soc. Am.* A **4**, 683–693.

Chang, D. C. & Kuester, E. F. 1976 *Radio Sci.* **11**, 449–457.

Collin, R. E. 1960 *Field theory of guided waves*. New York: McGraw-Hill.

Fang, X. S. & Lin, Z. Q. 1985*a* *IEEE J. Lightwave Technol.* **LT-3**, 789–794.

Fang, X. S. & Lin, Z. Q. 1985*b* *IEEE Trans. Microwave Theory Techniques.* **MTT-33**, 1150–1154.

Gambling, W. A., Payne, D. N. & Matsumura, H. 1976 *Electron. Lett.* **12**, 567–569.

Gambling, W. A. & Matsumura, H. 1977 *Electron. Lett.* **13**, 691–693.

Gambling, W. A. & Matsumura, H. 1978*a* *Opt. quantum Electron.* **10**, 31–40.

Gambling, W. A., Matsumura, H. & Ragdale, C. M. 1978*b* *Electron. Lett.* **14**, 130–132.

Gambling, W. A., Matsumura, H. & Ragdale, C. M. 1979 *Opt. quantum Electron.* **11**, 43–59.

Gloge, D. 1972 *Appl. Opt.* **11**, 2506–2513.

Jones, D. S. 1966 *Generalised functions*. London: McGraw-Hill.

Kraus, J. D. 1950 *Antennas*. New York: McGraw-Hill.

Lewin, L. 1974 *IEEE Trans. Microwave Theory Techniques* **MTT-22**, 718–727.

Lewin, L., Chang, D. C. & Kuester, E. F. 1977 *Electromagnetic waves and curved structure*, ch. 1. Stevenage: Peter Peregrinus.

Love, J. D. & Snyder, A. W. 1987 *Electron. Lett.* **23**, 1109–1110.

Marcatili, E. A. J. 1969 *Bell System tech. J.* **48**, 2103–2132.

Marcuse, D. 1972 *Light transmission optics*, ch. 9. New York: Van Nostrand Reinhold.

Marcuse, D. 1976*a* *J. opt. Soc. Am.* **66**, 216–220.

Marcuse, D. 1976*b* *J. opt. Soc. Am.* **66**, 311–320.

Miyagi, M. & Yip, G. L. 1976 *Opt. quantum Electron.* **8**, 335–341.

Moon, P. & Spencer, D. E. 1965 *Vectors*. Princeton: D. Van Nostrand.

Shevchenko, V. V. 1971 *Radiophys. quantum Electron.* **14**, 607–614.

Snyder, A. W. & Love, J. D. 1983 *Optical waveguide theory*, ch. 23. London: Chapman & Hall.

Stratton, J. A. 1941 *Electromagnetic theory*, ch. 1. New York: McGraw-Hill.

Tang, C. H. 1970 *IEEE Trans. Microwave Theory Techniques* **MTT-18**, 69.

Whittaker, E. T. & Watson, G. N. 1935 *A course of modern analysis*, 4th ed. Cambridge University Press.